Regularization Algorithm for Eliminating Singularities in the PIES Formula for 3D Multidomain Orthotropic Problems

Krzysztof Szerszeń [0000-0001-9256-2622] and Eugeniusz Zieniuk [0000-0002-6395-5096]

University of Bialystok, Institute of Computer Science
15-245 Białystok, Konstantego Ciołkowskiego 1M, Poland
k.szerszen@uwb.edu.pl, e.zieniuk@uwb.edu.pl

Abstract. This paper presents an algorithm designed to eliminate the direct evaluation of both strongly and weakly singular boundary integrals in the Parametric Integral Equation System (PIES) for the analysis of three-dimensional multidomain orthotropic problems. The proposed method regularizes PIES by incorporating an auxiliary regularization functions with coefficients that effectively remove singularities. Consequently, the regularized PIES eliminates the need to explicitly evaluate singular integrals, enabling all integrals to be computed using standard Gaussian quadrature.

Keywords: Regularized PIES, Singular Boundary Integrals, 3D Boundary Value Problems, Subdomains, Orthotropy, Bézier Surface Patches

1 Introduction

The computational analysis of various engineering problems often relies on well-established methods such as the Finite Element Method (FEM) [1] and the Boundary Element Method (BEM) [2]. In the authors' research, an alternative method to FEM and BEM was developed to eliminate the need for discretizing both the domain and its boundary. This was achieved through an analytical modification of the traditional Boundary Integral Equation (BIE) and the formulation of a Parametric Integral Equation System (PIES) [3]. The PIES enables direct incorporation of the boundary shape into the BIE formulation through parameterized functions, thereby eliminating the need for boundary discretization in numerical computations. This approach enables a more efficient and continuous representation of the problem domain. In PIES, the boundary is globally defined using a small set of control points, and in 3D problems, it is represented by parametric surface patches.

Although the analytical modification of BIE and the development of PIES introduced significant improvements, they did not eliminate the presence of singular integrals. As in BIE, the integrals in PIES still exhibit both strong and weak singularities in their integrands, arising from the characteristics of the integrand functions. Over the years, various techniques have been developed to address these challenges within the

ICCS Camera Ready Version 2025
To cite this paper please use the final published version:
DOI: 10.1007/978-3-031-97635-3_9

Boundary Integral Equation (BIE) framework, including subdivision methods [4–6], analytical evaluation of nearly singular integrals [7–9], and specialized quadrature rules [10,11]. Despite their widespread application, identifying a universal approach for handling a broad range of singular integrals remains a significant challenge.

The paper proposes an algorithm that eliminates the need for directly computing boundary singular integrals in the PIES formulation through regularization. Extending previous work on homogeneous media [12,13], this study generalizes the approach to three-dimensional problems involving subdomains characterized by orthotropic material properties. The proposed regularization involves the use of auxiliary functions containing regularization coefficients designed to eliminate both weakly and strongly singular terms. Notably, this approach is independent of the boundary shape and specified boundary conditions, enhancing its versatility. To model subdomain boundaries, Bézier surface patches are used, providing a smooth and flexible representation. Test results demonstrate a significant improvement in solution accuracy after applying the proposed regularization.

2 PIES for subdomains with piecewise homogeneous properties of an orthotropic medium

We consider a three-dimensional potential problem in a piecewise homogeneous orthotropic medium, governed by the partial differential equation

$$k_{11}^{(i)}\frac{\partial^2 u}{\partial x_1^2} + k_{22}^{(i)}\frac{\partial^2 u}{\partial x_2^2} + k_{33}^{(i)}\frac{\partial^2 u}{\partial x_3^2} = 0. \tag{1}$$

Fig. 1 illustrates the domain Ω, consisting of three homogeneous subdomains Ω_i ($i = 1,2,3$), each characterized by orthotropic coefficients $k_{11}^{(i)}, k_{22}^{(i)}, k_{33}^{(i)}$.

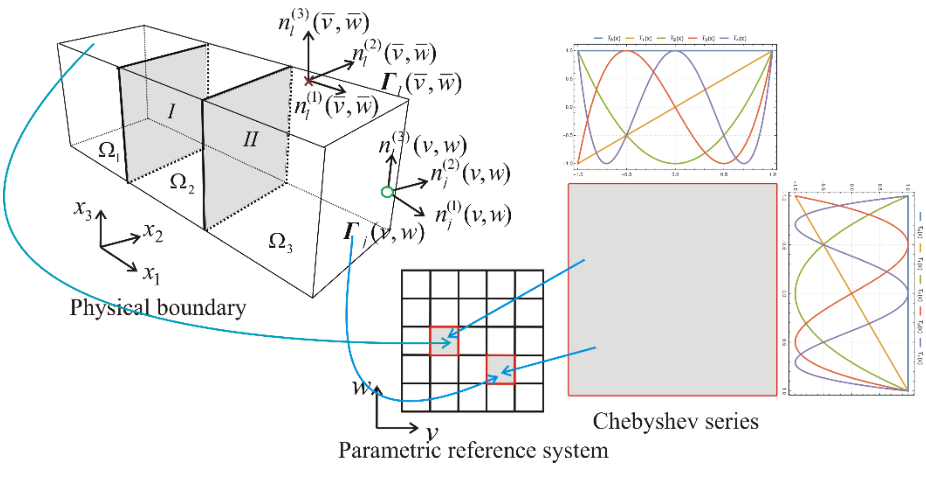

Fig. 1. Mapping of the boundary Γ of the domain Ω, consisting of homogeneous subdomains $\Omega_1, \Omega_2, \Omega_3$, onto a parameterized plane with boundary functions $u_j(v,w)$ and $p_j(v,w)$ approximated using Chebyshev series.

ICCS Camera Ready Version 2025
To cite this paper please use the final published version:
DOI: 10.1007/978-3-031-97635-3_9

PIES facilitates a one-dimensional mathematical reduction of the problem by evaluating it on the boundary, similar to BEM.However, unlike BEM, it maps the physical boundary onto a parameterized reference domain. In 3D, this involves projecting the boundary onto a parameterized plane, as shown in Fig. 1. The PIES formulation for each subdomain is given by

$$0.5u_l(\bar{v},\bar{w}) = \sum_{j=1}^{N}\int_{v_{j-1}}^{v_j}\int_{w_{j-1}}^{w_j}\{\bar{U}_{lj}^{*}(\bar{v},\bar{w},v,w)p_j(v,w) - \bar{P}_{lj}^{*}(\bar{v},\bar{w},v,w)u_j(v,w)\}J_j(v,w)dvdw, \tag{2}$$

where $v_{j-1} < \bar{v}, v < v_j,\ w_{j-1} < \bar{w}, w < w_j,\ l = 1,2,3, \dots, N.$

In equation (2), $u_j(v,w)$ and $p_j(v,w)$ represent the boundary functions, while $J_j(v,w)$ denotes the Jacobian of the transformation from the parametric domain to the Cartesian coordinate system. The boundary of each subdomain is defined using N parametric Bézier surface patches $\boldsymbol{\Gamma}_j(v,w)$. Fig. 1 depicts the boundary represented by 18 first-degree Bézier patches, with six patches per subdomain and two patches positioned along each shared interface. For more complex geometries, higher-degree patches can be employed. Each Bézier patch is directly embedded in the integrand functions of equation (2), as given by

$$\bar{U}_{lj}^{*}(\bar{v},\bar{w},v,w) = \frac{1}{4\pi\sqrt{k_{11}^{(i)}k_{22}^{(i)}k_{33}^{(i)}}}\frac{1}{\left(\eta_1^2/k_{11}^{(i)}+\eta_2^2/k_{22}^{(i)}+\eta_3^2/k_{33}^{(i)}\right)^{0.5}}, \tag{3}$$

$$\bar{P}_{lj}^{*}(\bar{v},\bar{w},v,w) = \frac{1}{4\pi\sqrt{k_{11}^{(i)}k_{22}^{(i)}k_{33}^{(i)}}}\frac{\eta_1 n_j^{(1)}(v,w)+\eta_2 n_j^{(2)}(v,w)+\eta_3 n_j^{(3)}(v,w)}{\left(\eta_1^2/k_{11}^{(i)}+\eta_2^2/k_{22}^{(i)}+\eta_3^2/k_{33}^{(i)}\right)^{1.5}}. \tag{4}$$

Here, η_{g} for $g = 1,2,3$ are defined as

$$\eta_{\mathrm{g}} = \Gamma_l^{(\mathrm{g})}(\bar{v},\bar{w}) - \Gamma_j^{(\mathrm{g})}(v,w), \tag{5}$$

where l and j denote the Bézier patches containing the source point (load point) and the field point (integration point), respectively. The terms $n_j^{(g)}(v,w)$ represent the components of the boundary normal vector, and the index g corresponds to the Cartesian coordinate directions, while the index i denotes the subdomain Ω_i. Moreover, we assume that the boundary functions $u_j(v,w)$ and $p_j(v,w)$ in (2) are expressed as Chebyshev series, taking the following form

$$u_j(v,w) = \sum_{p=0}^{P-1}\sum_{r=0}^{R-1}u_j^{(pr)}T_j^{(p)}(v)T_j^{(r)}(w), \tag{6}$$

$$p_j(v,w) = \sum_{p=0}^{P-1}\sum_{r=0}^{R-1}p_j^{(pr)}T_j^{(p)}(v)T_j^{(r)}(w), \tag{7}$$

where $u_j^{(pr)}$ and $p_j^{(pr)}$ represent the successive coefficients in these series. After obtaining $u_j(v,w)$ and $p_j(v,w)$ along the boundary using equation (2) by determining the values of the coefficients $u_j^{(pr)}$ and $p_j^{(pr)}$, the solution at any point within the computational domain can be determined by applying the integral identity within the subdomain Ω_i, as outlined in [3].

ICCS Camera Ready Version 2025
To cite this paper please use the final published version:
DOI: 10.1007/978-3-031-97635-3_9

3 Singularity removal in the PIES formulation via regularization

An analysis of equation (2) reveals a special case when $l = j$, meaning the load point and the integration point lie on the same patch. In such a case, as $v \to \bar{v}$ and $w \to \bar{w}$, the integrand function (3) becomes weakly singular, while (4) becomes strongly singular. This behavior arises from the fact that, under these conditions, the denominator in (3) and (4) approaches zero, hence the entire formulas tend toward infinity. To address this, equation (2) is transformed into an equivalent regularized form that eliminates these singularities. The procedure begins by replacing the boundary functions $u_j(v,w)$ and $p_j(v,w)$ in (2) with the auxiliary regularization functions (8) and (9), as described below

$$\breve{u}_j(v,w) = A_l(\bar{v},\bar{w})\left[\frac{\Gamma_l^{(1)}(\bar{v},\bar{w})-\Gamma_j^{(1)}(v,w)}{k_{11}^{(i)}} + \frac{\Gamma_l^{(2)}(\bar{v},\bar{w})-\Gamma_j^{(2)}(v,w)}{k_{22}^{(i)}} + \frac{\Gamma_l^{(3)}(\bar{v},\bar{w})-\Gamma_j^{(3)}(v,w)}{k_{33}^{(i)}}\right] + B_l(\bar{v},\bar{w}), \quad (8)$$

$$\breve{p}_j(v,w) = A_l(\bar{v},\bar{w})\left[n_j^{(1)}(v,w) + n_j^{(2)}(v,w) + n_j^{(3)}(v,w)\right]. \quad (9)$$

These functions satisfy (1) and depend on the geometry, boundary normals, material properties and the unknown regularization coefficients $A_l(\bar{v},\bar{w})$, $B_l(\bar{v},\bar{w})$. Next, subtracting equation (2) with $\breve{u}_j(v,w)$ and $\breve{p}_j(v,w)$ from the original version with $u_j(v,w)$ and $p_j(v,w)$, we obtain

$$0.5\{u_l(\bar{v},\bar{w}) - B_l(\bar{v},\bar{w})\} = \sum_{j=1}^{N}\int_{v_{j-1}}^{v_j}\int_{w_{j-1}}^{w_j}\Bigg\{\bar{U}_{lj}^*(\bar{v},\bar{w},v,w)\Big\{p_j(v,w) - A_l(\bar{v},\bar{w})\left[n_j^{(1)}(v,w) + n_j^{(2)}(v,w) + n_j^{(3)}(v,w)\right]\Big\} - \bar{P}_{lj}^*(\bar{v},\bar{w},v,w)\Big\{u_j(v,w) - A_l(\bar{v},\bar{w})\left[\frac{\Gamma_l^{(1)}(\bar{v},\bar{w})-\Gamma_j^{(1)}(v,w)}{k_{11}^{(i)}} + \frac{\Gamma_l^{(2)}(\bar{v},\bar{w})-\Gamma_j^{(2)}(v,w)}{k_{22}^{(i)}} + \frac{\Gamma_l^{(3)}(\bar{v},\bar{w})-\Gamma_j^{(3)}(v,w)}{k_{33}^{(i)}}\right] + B_l(\bar{v},\bar{w})\Big\}\Bigg\}J_j(v,w)dvdw. \quad (10)$$

At the singular point ($l = j$, $v = \bar{v}$, $w = \bar{w}$) the singularities in (3) and (4) are removed by choosing

$$A_l(\bar{v},\bar{w}) = \frac{p_l(\bar{v},\bar{w})}{n_l^{(1)}(\bar{v},\bar{w})+n_l^{(2)}(\bar{v},\bar{w})+n_l^{(3)}(\bar{v},\bar{w})}, \quad (11)$$

$$B_l(\bar{v},\bar{w}) = u_l(\bar{v},\bar{w}). \quad (12)$$

By substituting equations (11) and (12) into (10), the final regularized PIES formulation is obtained, as presented below

ICCS Camera Ready Version 2025
To cite this paper please use the final published version:
DOI: 10.1007/978-3-031-97635-3_9

$$\begin{aligned}
&\sum_{j=1}^{N}\left\{\int_{v_{j-1}}^{v_j}\int_{w_{j-1}}^{w_j}\bar{U}_{lj}^{*}(\bar{v},\bar{w},v,w)\left[p_j(v,w)-\frac{n_j^{(1)}(v,w)+n_j^{(2)}(v,w)+n_j^{(3)}(v,w)}{n_l^{(1)}(\bar{v},\bar{w})+n_l^{(2)}(\bar{v},\bar{w})+n_l^{(3)}(\bar{v},\bar{w})}p_l(\bar{v},\bar{w})\right]-\right.\\
&\int_{v_{j-1}}^{v_j}\int_{w_{j-1}}^{w_j}\bar{P}_{lj}^{*}(\bar{v},\bar{w},v,w)\left[-\frac{\frac{\Gamma_l^{(1)}(\bar{v},\bar{w})-\Gamma_j^{(1)}(v,w)}{k_{11}^{(i)}}+\frac{\Gamma_l^{(2)}(\bar{v},\bar{w})-\Gamma_j^{(2)}(v,w)}{k_{22}^{(i)}}+\frac{\Gamma_l^{(3)}(\bar{v},\bar{w})-\Gamma_j^{(3)}(v,w)}{k_{33}^{(i)}}}{n_l^{(1)}(\bar{v},\bar{w})+n_l^{(2)}(\bar{v},\bar{w})+n_l^{(3)}(\bar{v},\bar{w})}p_l(\bar{v},\bar{w})+\right.\\
&\left.\left.u_j(v,w)-u_l(\bar{v},\bar{w})\right]\right\}J_j(v,w)\,dv\,dw=0. \qquad (13)
\end{aligned}$$

Thanks to the regularization, all integrals in equation (13) become nonsingular.

4 Subdomain Assembly

For computational purposes, the boundary functions are approximated using Chebyshev series (6,7). The use of Chebyshev series allows for systematic improvement in accuracy by increasing the number of terms. The collocation method is then applied to solve equation (13) to obtain the values of the coefficient $u_j^{(pr)}$ and $p_j^{(pr)}$. In handling multiple interconnected subdomains, matrix elements must be defined on both external and interface boundaries. For each of the three subdomains shown in Fig. 1, separate systems of algebraic equations can be formulated based on the PIES in the following form

for Ω_1
$$\begin{bmatrix} H_{\Gamma_1} & H_{\Gamma_{1I}} \end{bmatrix}\begin{bmatrix} p_{\Gamma_1} \\ p_{\Gamma_{1I}} \end{bmatrix}=\begin{bmatrix} G_{\Gamma_1} & G_{\Gamma_{1I}} \end{bmatrix}\begin{bmatrix} u_{\Gamma_1} \\ u_{\Gamma_{1I}} \end{bmatrix}, \qquad (14)$$

for Ω_2
$$\begin{bmatrix} H_{\Gamma_{2I}} & H_{\Gamma_2} & H_{\Gamma_{2II}} \end{bmatrix}\begin{bmatrix} p_{\Gamma_{2I}} \\ p_{\Gamma_2} \\ p_{\Gamma_{2II}} \end{bmatrix}=\begin{bmatrix} G_{\Gamma_{2I}} & G_{\Gamma_2} & G_{\Gamma_{2II}} \end{bmatrix}\begin{bmatrix} u_{\Gamma_{2I}} \\ u_{\Gamma_2} \\ u_{\Gamma_{2II}} \end{bmatrix}, \qquad (15)$$

for Ω_3
$$\begin{bmatrix} H_{\Gamma_{3II}} & H_{\Gamma_3} \end{bmatrix}\begin{bmatrix} p_{\Gamma_{3II}} \\ p_{\Gamma_3} \end{bmatrix}=\begin{bmatrix} G_{\Gamma_{3II}} & G_{\Gamma_3} \end{bmatrix}\begin{bmatrix} u_{\Gamma_{3II}} \\ u_{\Gamma_3} \end{bmatrix}. \qquad (16)$$

Here, $\Gamma_1, \Gamma_2, \Gamma_3$ denote external boundaries, while Γ_{1I}, Γ_{2I} and $\Gamma_{2II}, \Gamma_{3II}$ refer to interface boundaries I and II, respectively. To assemble the global system, continuity and equilibrium conditions must be enforced on the shared boundaries, as outlined below

$$u_{\Gamma_{1I}}=u_{\Gamma_{2I}}=u_{\Gamma_I},\ p_{\Gamma_{1I}}=-p_{\Gamma_{2I}}=p_{\Gamma_{II}},\ u_{\Gamma_{2II}}=u_{\Gamma_{3II}}=u_{\Gamma_{II}},\ p_{\Gamma_{2II}}=-p_{\Gamma_{3II}}=p_{\Gamma_{II}}. \qquad (17)$$

Combining (14-16) with the compatibility conditions (17) yields the global system

$$\begin{bmatrix} H_{\Gamma_1} & H_{\Gamma_{1I}} & -G_{\Gamma_{1I}} & 0 & 0 & 0 & 0 \\ 0 & H_{\Gamma_{2I}} & -G_{\Gamma_{2I}} & H_{\Gamma_2} & H_{\Gamma_{2II}} & -G_{\Gamma_{2II}} & 0 \\ 0 & 0 & 0 & 0 & H_{\Gamma_{3II}} & -G_{\Gamma_{3II}} & H_{\Gamma_3} \end{bmatrix}\begin{bmatrix} p_{\Gamma_1} \\ u_{\Gamma_I} \\ p_{\Gamma_I} \\ p_{\Gamma_2} \\ u_{\Gamma_{II}} \\ p_{\Gamma_{II}} \\ p_{\Gamma_3} \end{bmatrix}=\begin{bmatrix} G_{\Gamma_1} & 0 & 0 \\ 0 & G_{\Gamma_2} & 0 \\ 0 & 0 & G_{\Gamma_3} \end{bmatrix}\begin{bmatrix} u_{\Gamma_1} \\ u_{\Gamma_2} \\ u_{\Gamma_3} \end{bmatrix}. \qquad (18)$$

ICCS Camera Ready Version 2025
To cite this paper please use the final published version:
DOI: 10.1007/978-3-031-97635-3_9

The dimensions of the matrices in (18) depend on the number of Bézier surface patches used to model the boundary and the number of Chebyshev terms per patch.

5 Results

5.1 Example 1

We return to the domain shown in Fig. 1, consisting of three subdomains $\Omega_1, \Omega_2, \Omega_3$. We assume that all three subdomains share identical parameters for the orthotropic medium $k_{11} = k_{22} = 0.5$ and $k_{33} = 2$. Defining the boundaries of these subdomains requires specifying 18 interconnected Bézier patches of the first degree, defined by 16 corner points. We assume that the expected field distribution on the boundary and inside the domains is described by the following function depending on the Cartesian coordinates $\boldsymbol{x} = \{x_1, x_2, x_3\}$ and satisfying the the equation (1)

$$u_A(x_1, x_2, x_3) = 2x_1^2 + 2x_2^2 - x_3^2. \tag{19}$$

Dirichlet boundary conditions are specified on each surface patch defining the boundary, based on this function. The problem is solved using both the singular (2) and regularized (13) PIES formula on the boundary. The singularity appearing in (2) results from its mathematical formula, as indicated at the beginning of section 3 of the paper. Accuracy is assessed at internal points, with relative errors shown in Table 1.

Table 1. Relative error [%] at selected points for Example 1.

(x_1, x_2, x_3)	Analytical (19)	PIES (2) [%]	PIES (13) [%]
(5.5,0.25,1.0)	60.125	0.903981	0.061675
(4.5,0.5,1.0)	40.500	0.303981	0.024603
(3.5,0.25,1.0)	24.125	0.180077	0.011574
(2.5,0.25,1.0)	12.125	0.129525	0.009263
(1.5,0.25,1.0)	4.125	0.102096	0.008490
(0.25, 0.25,1.0)	-0.250	0.106148	0.000548

The obtained results indicate a significant improvement in the accuracy of the solutions obtained using the proposed regularization approach compared to the singular variant of PIES.

5.2 Example 2

In the next example, we extend the analysis of the field distribution defined by (19) to a new domain, shown in Fig. 2, described by both flat and curved Bézier patches. This domain is divided into two subdomains, Ω_1 and Ω_2. The subdomain boundaries are represented by 7 cubic Bézier patches for the curvilinear segments and 9 linear Bézier patches. Defining the complete boundary with 16 patches required specifying 112 control points.

ICCS Camera Ready Version 2025
To cite this paper please use the final published version:
DOI: 10.1007/978-3-031-97635-3_9

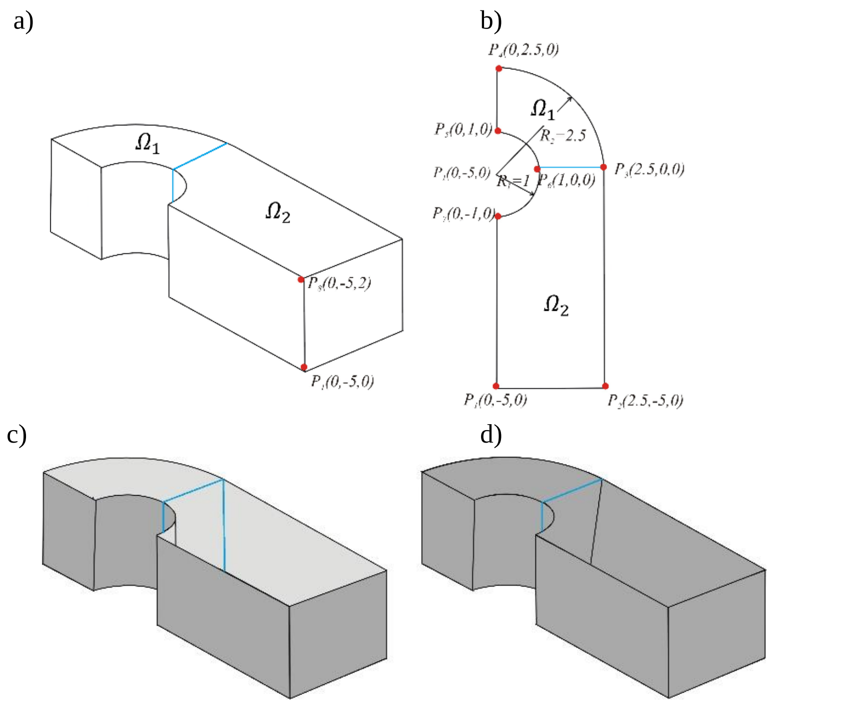

Fig. 2. Modeling of subdomains using Bézier patches: the domain contour in a 3D view (a) and the projection of the lower base, with the subdomains Ω_1, Ω_2 (b); the defined base of the subdomains using 2 cubic Bézier patches and 1 linear patch, along with the side walls of the domains modeled with 3 cubic Bézier patches and 8 linear patches (c); and the complete boundary definition of the subdomains (d).

It is assumed that both subdomains Ω_1, Ω_2, have identical properties with the following parameters for the orthotropic medium $k_{11} = k_{22} = 0.5$ and $k_{33} = 2$. The Dirichlet boundary conditions are again obrained from (19). Table 2 presents a comparison of the relative errors for solutions obtained at selected points within the subdomains Ω_1 and Ω_2 with help of (2) and (13).

Table 2. Relative error of the solutions at selected points within the subdomains for Example 2.

(x_1, x_2, x_3)	Analytical (19)	PIES (2) [%]	PIES (13) [%]
(0.862,1.690,0.926)	6.34442	0.03376	0.00673
(0.536,-2.136,0.409)	9.53990	0.05628	0.00215
(0.949,-3.754,1.528)	27.6615	0.07986	0.00145
(1.237,-2.989,1.656)	18.1899	0.01701	0.00162
(0.573,-1.741,1.278)	5.08737	0.01459	0.00268
(1.491,-2.870,1.648)	18.21070	0.01211	0.00677
(0.779,-2.090,0.460)	9.73909	0.02113	0.00232

Once again, this example demonstrates a clear improvement in the solutions obtained using the regularized formula (13).

ICCS Camera Ready Version 2025
To cite this paper please use the final published version:
DOI: 10.1007/978-3-031-97635-3_9

6 Conclusions

This paper presents an algorithm that eliminates the need for direct evaluation of both strongly and weakly singular boundary integrals within the PIES, enabling efficient analysis of three-dimensional, multidomain orthotropic problems. Notably, all integrals are computed numerically, removing the requirement for analytical evaluation. Once regularized, these integrals can be accurately evaluated using standard Gaussian quadrature. The proposed method preserves all the established advantages of PIES in homogeneous regions. These benefits include a simplified subdomain representation - achieved with minimal input data and the decoupling of boundary geometry, defined via surface patches, from the approximation of boundary functions using Chebyshev series. The preliminary verification of the proposed approach, as presented in this work, will be extended in future research through a comparative analysis with other numerical methods, focusing on computational efficiency, accuracy and execution time.

References

1. Zienkiewicz, O. C., Taylor, R. L., Zhu, J. Z.: The finite element method: its basis and fundamentals. Elsevier (2005).
2. Brebbia, C. A., Telles, J. C. F., Wrobel, L. C.: Boundary element techniques: theory and applications in engineering. Springer Science & Business Media (2012).
3. Zieniuk, E., Szerszen, K.: The PIES for solving 3D potential problems with domains bounded by rectangular Bézier patches. Engineering Computations, 31(4), 791-809 (2014).
4. Scuderi, L.: On the computation of nearly singular integrals in 3D BEM collocation. International Journal for Numerical Methods in Engineering 74, 1733-1770 (2008).
5. Gao, X. et al.: An adaptive element subdivision technique for evaluation of various 2D singular boundary integrals. Engineering Analysis with Boundary Elements 32, 692-696 (2008).
6. Zhang, J. et al.: A binary-tree subdivision method for evaluation of singular integrals in 3D BEM. Engineering Analysis with Boundary Elements, 103, 80-93 (2019).
7. Niu, Z. et al.: Analytic formulations for calculating nearly singular integrals in two-dimensional BEM. Engineering Analysis with Boundary Elements 31, 949-964 (2007).
8. Zhou, H. et al.: Analytical integral algorithm applied to boundary layer effect and thin body effect in BEM for anisotropic potential problems. Computers & Structures, 86, 1656-1671 (2008).
9. Ren, Q., and Chan, C.L.: Analytical evaluation of the BEM singular integrals for 3D Laplace and Stokes flow equations using coordinate transformation. Engineering Analysis with Boundary Elements, 53, 1-8 (2015).
10. Lutz, E.: Exact Gaussian quadrature methods for near-singular integrals in the boundary element method. Engineering Analysis with Boundary Elements 9, 233-245 (1992).
11. Tausch, J.: Adaptive quadrature rules for Galerkin BEM. Computers & Mathematics with Applications, 113, 270-281 (2022).
12. Zieniuk, E., Szerszeń, K.: Near corner boundary regularization of the parametric integral equation system (PIES). Engineering Analysis with Boundary Elements, 158, 51-67 (2024).
13. Szerszeń K., Zieniuk E.: Elimination of computing singular surface integrals in the PIES method through regularization for three-dimensional potential problems. International Conference on Computational Science ICCS 2024, Lecture Notes of Computer Science 14833, Part II, 325-338 (2024).

ICCS Camera Ready Version 2025
To cite this paper please use the final published version:
DOI: 10.1007/978-3-031-97635-3_9